(15) NGR-09-010-085

(6) A NEW CAPABILITY FOR PREDICTING HELICOPTER ROTOR NOISE IN HOVER AND IN FLIGHT

(11) 1976

(12) 14 p.

(10) THOMAS J. BROWN, MP
FEREIDOUN FARASSAT, [illegible].
USAAMRDL, VJIAFS, LANGLEY RESEARCH CENTER
HAMPTON, VIRGINIA 23665

The problem of noise radiation from helicopter rotors has gained prominence due to its annoyance to the public and detectability. Although the rotor is one of the several noise generating sources of helicopters, it is the most important in the external regions of the present machines. Clearly, the reliable prediction of this noise in the design stage of the rotor is an important step in controlling the level of the noise intensity. There has been a steady advance in the last decade in the prediction of rotor noise (ref. 1). There are still disagreements between the theoretical and experimental results of rotor acoustics. In addition to this shortcoming, the available theories suffer from a combination of the following restrictions:

a. Compactness of the acoustic sources
b. Hovering helicopter
c. Observer in the far field
d. Limited airfoil shapes
e. Limited surface pressure distribution models
f. Singularities in the solution for high rotor tip speeds
g. Neglect of the thickness noise

It is believed that the removal of these restrictions and the inclusion of the nonlinear propagation effects should result in reliable prediction of the rotor noise.

Traditionally, rotor noise has been divided into several categories such as rotational, vortex and thickness noise. These can be grouped into two broad classes — those depending on the local

pressure and viscous stress distribution on the rotor blades and those due to the normal velocity distribution on the blades. For example, rotational noise belongs to the first class and thickness noise to the second. A theory which incorporates the effects of surface pressure and normal velocity distribution on a moving body is developed in reference 2. The formulation is then specialized for propellers and helicopter rotors. In this work a study of compactness assumption of sources on moving bodies has revealed that in the case of helicopter rotors and propellers, the sources on the blades cannot be considered compact for the observer position in a large region of space around the rotor. If the compactness restriction is removed, then one would like to remove the restrictions of limited airfoil shapes and surface pressure distribution models to improve the prediction technique.

The present paper discusses a new computer program developed by the authors at NASA Langley Research Center based on the results of reference 2. The purpose of developing this program has been to remove the restrictions of the already existing theories and thus achieve a new capability in the prediction of the rotor and propeller noise. The acoustic computation is performed in the time domain and the resulting pressure signature is then Fourier analyzed to get the acoustic pressure spectrum.

Examples are presented in this paper to demonstrate the capabilities of this new program. These examples are selected mainly with regard to the restrictions discussed earlier which are removed by the new formulation.

THE ACOUSTIC FORMULATION

The formulation derived in reference 2 is briefly discussed here. Consider a moving body whose surface is described by $f(\vec{y}, \tau) = 0$ where τ is the source time. Let V_n be the local normal velocity of the surface, the acoustic pressure $p(\vec{x}, t)$ is given by

$$4\pi p(\vec{x}, t) = \frac{\partial}{\partial t} \int_{\tau_1}^{\tau_2} \int_{\Gamma} \frac{\rho_o c V_n + p \cos\theta}{r \sin\theta} \, d\Gamma \, d\tau$$

$$+ c \int_{\tau_1}^{\tau_2} \int_{\Gamma} \frac{p \cot\theta}{r^2} \, d\Gamma \, d\tau \qquad (1)$$

Where

$\vec{x}$, t: observer position and time

c: speed of sound in undisturbed medium

ρ_o: density of the undisturbed medium

r: $|\vec{x} - \vec{y}|$, $\vec{y}$ source location on the body

θ: the angle between radiation direction $\vec{r} = \vec{x} - \vec{y}$ and the outward normal to the body

p: (under the integral) the surface pressure on the body

Γ: the curve of the intersection of the collapsing sphere $g = \tau - t + r/c = 0$ and the body $f(\vec{y}, \tau) = 0$

τ_1, τ_2: the times when the sphere $g = 0$ enters and leaves the body, respectively

For application to rotors and propellers, the above equation will be rewritten in the form given below. Let a new frame η' be fixed to each blade such that $\eta_1' \eta_2'$-plane contains the rotor disk and η_2'-axis is along the span of the blade. Let $\eta_3' = T(\eta_1', \eta_2')$ and $\eta_3' = h(\eta_1', \eta_2')$ be the equations of the thickness distribution and camber surface, respectively. The components of unit radiation vector $(\vec{x} - \vec{y})/r$ and the vehicle velocity $\vec{V}$ in this rotating frame will be denoted by $(\hat{r}_1', \hat{r}_2', \hat{r}_3')$ and (V_1', V_2', V_3'), respectively. Equation (1) can be written as follows (ref. 2):

$$p(\vec{x}, t) = \frac{\partial}{\partial t}\,[I_1 + I_2 + I_3] + I_4 + I_5 \tag{3}$$

The expressions for I_1 to I_5 are

$$I_1 = \frac{\rho_o c}{4\pi} \int_{\tau_1}^{\tau_2} \int_{\Gamma(Dp)} \frac{L_1 \tilde{V}_1' + L_2 \tilde{V}_2'}{rD}\, d\Gamma\, d\tau \tag{4}$$

$$I_2 = -\frac{1}{4\pi} \int_{\tau_1}^{\tau_2} \int_{\Gamma(Dp)} \frac{\Delta p \cos\theta_n}{rD}\, d\Gamma\, d\tau \tag{5}$$

$$I_3 = -\frac{1}{2\pi}\int_{\tau_1}^{\tau_2}\int_{\Gamma(Dp)} \frac{p_T\,(T_1\,\hat{r}_1' + T_2\,\hat{r}_2')}{rD}\,d\Gamma\,d\tau \qquad (6)$$

$$I_3 = -\frac{1}{4\pi}\int_{\tau_1}^{\tau_2}\int_{\Gamma(Dp)} \frac{\Delta p\,\cos\theta_h}{r^2 D}\,d\Gamma\,d\tau \qquad (7)$$

$$I_5 = -\frac{1}{2\pi}\int_{\tau_1}^{\tau_2}\int_{\Gamma(Dp)} \frac{p_T\,(T_1\,\hat{r}_1' + T_2\,\hat{r}_2')}{r^2 D}\,d\Gamma\,d\tau \qquad (8)$$

The symbols used in the above expressions have the following meaning:

Dp: disk plane

T_1, T_2: $\frac{\partial T}{\partial \eta_1'}$, $\frac{\partial T}{\partial \eta_2'}$, respectively

$\tilde{V}_1'$: $-V_1' + \eta_2'\Omega$

$\tilde{V}_2'$: $-V_2' - \eta_1'\Omega$

Ω: rotor angular velocity

D: $[1 - \hat{r}_3'^2 + T_1^2\,(1 - \hat{r}_1'^2)]^{1/2}$

Δp: local pressure differential producing the lift distribution

p_T: pressure distribution on the blade due to thickness distribution alone

θ_h: the angle between the upward normal to the camber surface and the radiation direction

Note that in equations (4) to (8), the integrations are carried out once along the arc of intersection of the collapsing sphere $g = 0$ and the projection of the blade planforms in the disk plane.

COMPUTATIONAL METHOD

Equations (4) to (6) are evaluated on a computer using a double numerical integration followed by numerical smoothing and differentiation where required. Each of the five terms are integrated separately. The first three are subsequently differentiated and the resulting five pressure contributions are added to obtain the pressure signature and spectrum.

At source $\tau = \tau_j$ a sphere is constructed with its center at the observer location. Its radius R_j is selected such that its circle of intersection, C', in the plane of the rotor is tangent to the rotor disk. From this initial geometry the initial observer time, t_j, is calculated from $t_j = \tau_j + R_j/c$ where c is the speed of sound in the medium. The sphere is allowed to collapse by an amount $c\Delta\tau$, where τ is the emission or source time. During this period, the helicopter rotor is allowed to translate and rotate. The resulting arc of intersection between the rotor disk and the new C' is swept point by point in a counterclockwise direction until an intersection with a blade surface is detected or until the arc passes out of the rotor disk. When a blade is encountered, the integrands of equations (4) to (6) are evaluated and subsequently the line integrals are accumulated point by point using a trapezoidal scheme.

The collapsing process of the sphere $g = 0$ is repeated, each time yielding a value for the line integrals which are accumulated for the source time integration using simpson rule. This process is continued until it is detected that the collapsing sphere has passed out of the rotor disk. The integration is thus concluded for the observer time t_j and the resulting integrals are saved for further processing. Successive points are obtained in like manner.

To facilitate numerical smoothing and differentiation with respect to the observer time t, it is required that the t_j's be equally spaced. Since the relation between the observer time t and the source time τ is in general nonlinear, an iteration technique is used to obtain the initial radius R_j and the corresponding source time τ_j where the sphere $g = 0$ begins to collapse. The smoothing and numerical differentiation which is used are presented in reference 3. It is based on the theory of finite Fourier series using sigma factors to improve convergence characteristics and to reduce Gibbs phenomenon. As a byproduct of this, the pressure spectrum of the acoustic signature is obtained quite easily using intermediate results of the smoothing and differentiation process.

EXAMPLES DEMONSTRATING UNIQUE FEATURES

The following examples are selected with realistic data to demonstrate the unique features of the developed program. Rectangular blade planform is used in all examples. This is one of the limitations of the present program which will be removed in future.

In the first two examples, the two-bladed rotor system is 4.58 m in diameter and has a chord of 0.356 m. For the first example, the blade has an NACA four-digit airfoil section of 12 percent thickness ratio. The tip speed is 151.3 m/sec. The pressure distribution Δp corresponding to this tip speed was measured by Rabbott (ref. 4) for various angles of attack. The angle of attack here is 8.5°. The chordwise pressure distribution has a maximum at leading edge and the spanwise loading has the familiar variation of increasing towards tip and reaching a maximum at about 90 percent of the radius. For this example, a function of two variables approximating the pressure distribution in the outer 40 percent of the radius was first obtained and was used as an input to the program. The pressure p_T due to the symmetric thickness distribution was also obtained analytically using the data given in reference 5 and corrected for compressibility effect by Prandtl-Glauret rule. The observer is 10 m from the center of the rotation and 45° above the rotor plane. The theoretical pressure signature and the pressure spectrum are presented in Figure 1. The shape of the pressure signature is considerably influenced by the thickness noise even for such a high observer elevation. This was found to be true for blades with blunt leading edge. In this and all the examples worked out so far, the contribution of the expression $\frac{\partial I_3}{\partial t}$ (see eq. (6)), was found to be of the order of 10 percent of the thickness noise due to $\frac{\partial I_1}{\partial t}$. This is expected on theoretical basis. The contributions of expressions I_4 and I_5 are very small compared to the other terms except very close to the blades.

The second example has rotor tip speed of 259 m/sec (Tip Mach number = 0.75). To utilize the measured data of reference 4, a similarity rule is applied to the blades of the first example. To obtain the same pressure coefficient c_p as in the above case, the thickness ratio varies along span by the following rule (ref. 6).

$$\frac{\text{thickness ratio}}{\sqrt{1 - M_2^2}} = \frac{0.12}{\sqrt{1 - M_1^2}}$$

where $M_2 = \Omega_2 \tilde{r}/c$ and $M_1 = \Omega_1 \tilde{r}/c$ where Ω_1 and Ω_2 are the

angular velocities of the rotors of the first and second example, respectively, and $\tilde{r}$ is the spanwise distance from the rotor center. The angle of attack α in this example also varies along the span as follows:

$$\frac{\alpha}{\sqrt{1 - M_2^2}} = \frac{8.5}{\sqrt{1 - M_1^2}}$$

where α is in degrees. Again p_T from reference 5 was corrected for compressibility effect. The observer is 10 m from the rotor center and in the rotor plane. Figure 2 presents the pressure signature and the spectrum. The signature is again considerably influenced by the thickness noise.

The above two examples demonstrate the use of realistic pressure distributions, airfoils with blunt leading edge, and blade twist.

The third and fourth examples demonstrate that there is no limitation on tip Mach numbers. In these examples a two-bladed rotor of 10-meter diameter and a chord of 0.4 m is used. The blade length is 1 m and a biconvex wedge airfoil section of 6 percent thickness ratio is used. The angle of attack is 2.5°. The tip Mach number is 1.375. Linearized two-dimensional aerodynamic theory was used to calculate Δp and p_T which vary with spanwise location. Figure 3 gives the pressure signature and spectrum for the observer 50 m from rotor center and in the rotor plane. Figure 4 presents pressure signature and spectrum for the observer 50 m from rotor center but at 45° elevation above rotor plane. The changes in the signatures are striking but expected.

The fifth example demonstrates the forward flight capability of the program. The helicopter speed is 59.2 m/sec (115 kts). The rotor system is that of HU-1H which is 14.64 m in diameter and has a chord of 0.53 m. The rotor rpm is 324. The observer is 22.9 m from rotor center and 2° below the rotor plane. Due to unavailability of reliable surface pressure measurements, only the thickness noise is presented. However, it was found earlier that at high tip speeds and in or near the plane of rotation, thickness noise is dominant (ref. 7). This conclusion is born out by comparing the calculated pressure signature, figure 5, with the measured signature in reference 8. The peaks of the measured signature are higher in magnitude but the deviation is less than 2 db which is considered good agreement in acoustics. The exact effect of the inclusion of the expression involving Δp, which is believed to be important next to the thickness noise, cannot be determined at this stage.

CONCLUSIONS

The present paper discusses a new theory and a computer program for realistic calculation of acoustic pressure signature and spectrum of rotor and propeller noise. As seen from the examples in this paper, many of the common restrictions of already existing theories are removed using the new theory which is consistent with all previous theories. Only deterministic pressure fluctuations may be used in the program at this stage of development. This will limit the applicability of the program to relatively high tip speeds where it is known that high frequency unsteady pressure fluctuations do not contribute significantly to the sound level. There are very few blade surface pressure measurements and reliable acoustic data available to test the theory in full. Some comparison with experimental measurements has been given in reference 7 (using theoretical thickness noise). Further comparison with the measured acoustic data of a high-speed propeller by Hubbard and Lassiter (ref. 9) using limited aerodynamic data in the blade tip region for acoustic calculations, has shown good agreement so far. One important contribution of the new theory is believed to be the removal of the compactness assumption which can introduce errors in acoustic computations. The new capability will be used to study this effect. Already it has been found that in most cases of interest one only needs to keep the two expressions I_1 and I_2, and in some cases one of these two will give a good estimate of the acoustic pressure of the rotor. More numerical examples and comparison with experimental data are planned.

REFERENCES

1. Magliozzi, B., et al: A Comprehensive Review of Helicopter Noise Literature. Final Report, U.S. Dept. of Transportation, 1975.

2. Farassat, F.: Theory of Noise Generation From Moving Bodies with an Application to Helicopter Rotors. NASA TR R-451, December 1975.

3. Lanczos, C.: Applied Analysis. Prentice Hall, Inc., Englewood Cliffs, N. J., 1956.

4. Rabbott, J. P.: Static-Thrust Measurements of the Aerodynamic Loading on a Helicopter Rotor Blade. NACA Tech. Note 3688, 1956.

5. Abbott, I. H.; Von Doenhoff, A. E.: Theory of Wing Sections - Including a Summary of Airfoil Data. Dover Publications, Inc., New York, 1959.

6. Liepmann, H. W.; Roshko, A.: Elements of Gasdynamics. John Wiley and Sons, Inc., New York, 1957.

7. Farassat, F.; Pegg, R. J.; Hilton, D. A.: Thickness Noise of Helicopter Rotors at High Tip Speeds. AIAA Paper 75-453, March 1975.

8. Boxwell, D. A.; Schmitz, F. H.; Hanks, M. L.: In-Flight Far Field Measurement of Helicopter Impulsive Noise. Presented at the "First Rotorcraft and Powered Lift Aircraft Forum," University of Southampton, Southampton, England, September 22-24, 1975.

9. Hubbard, H. H.; Lassiter, L. W.: Sound From a Two-Blade Propeller at Supersonic Tip Speeds. NACA Tech. Report 1079, 1952.

ACKNOWLEDGEMENTS

The second author acknowledges the support from NASA Grant No. NGR-09-010-085, entitled "Aircraft Noise Reduction." The authors would like to thank Mrs. Christine G. Brown for her kind help in computations.

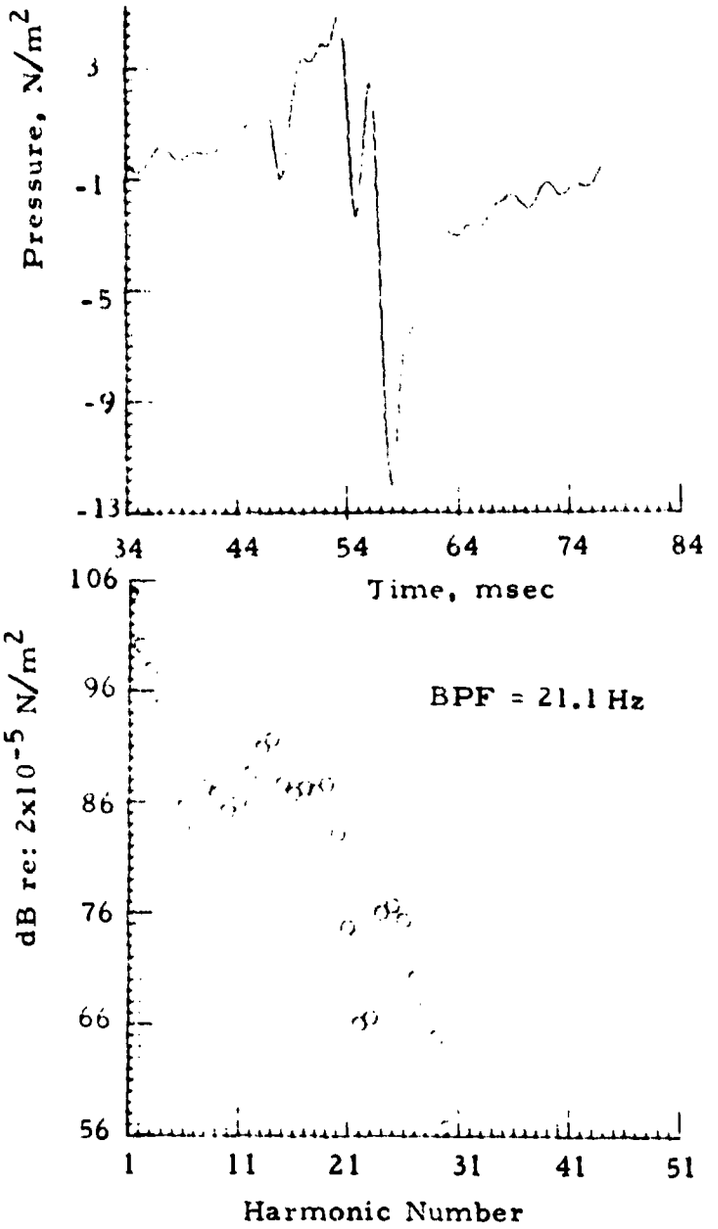

Figure 1. Example 1.- Theoretical acoustic pressure signature and spectrum of a hovering helicopter rotor for an observer at 45° elevation above rotor plane. Tip Mach number = 0.44.

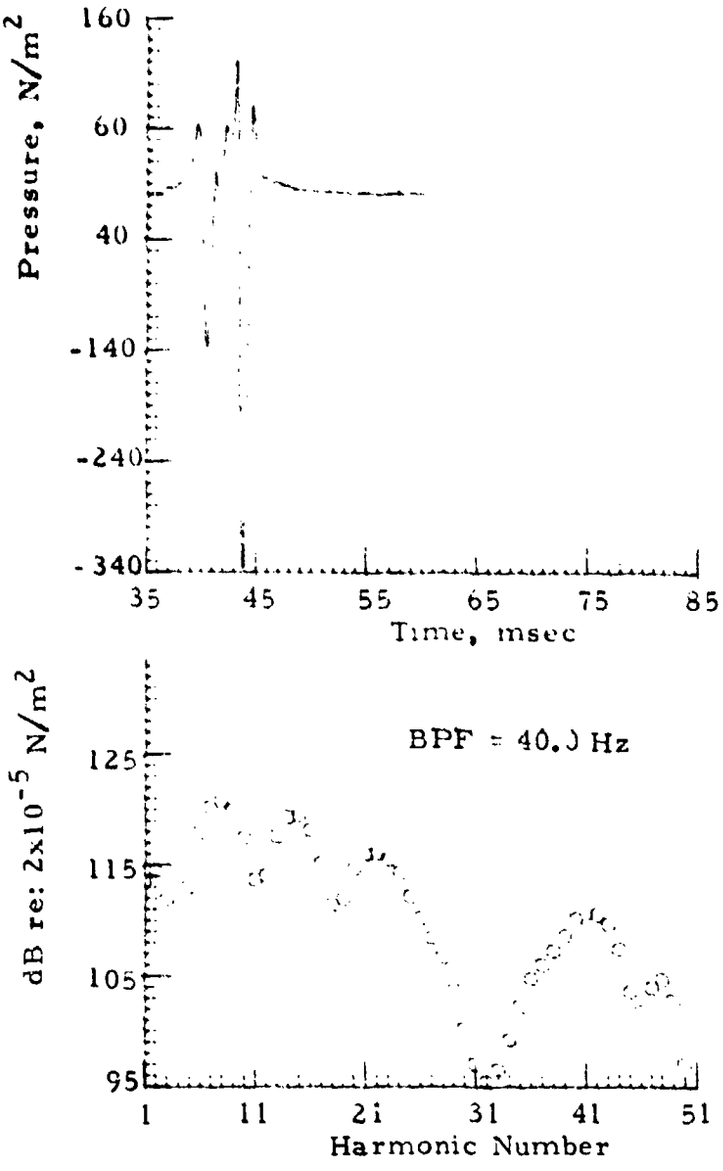

Figure 2. Example 2.- Theoretical acoustic pressure signature and spectrum of a hovering helicopter rotor for an observer in the plane of rotation. Tip Mach number = 0.75.

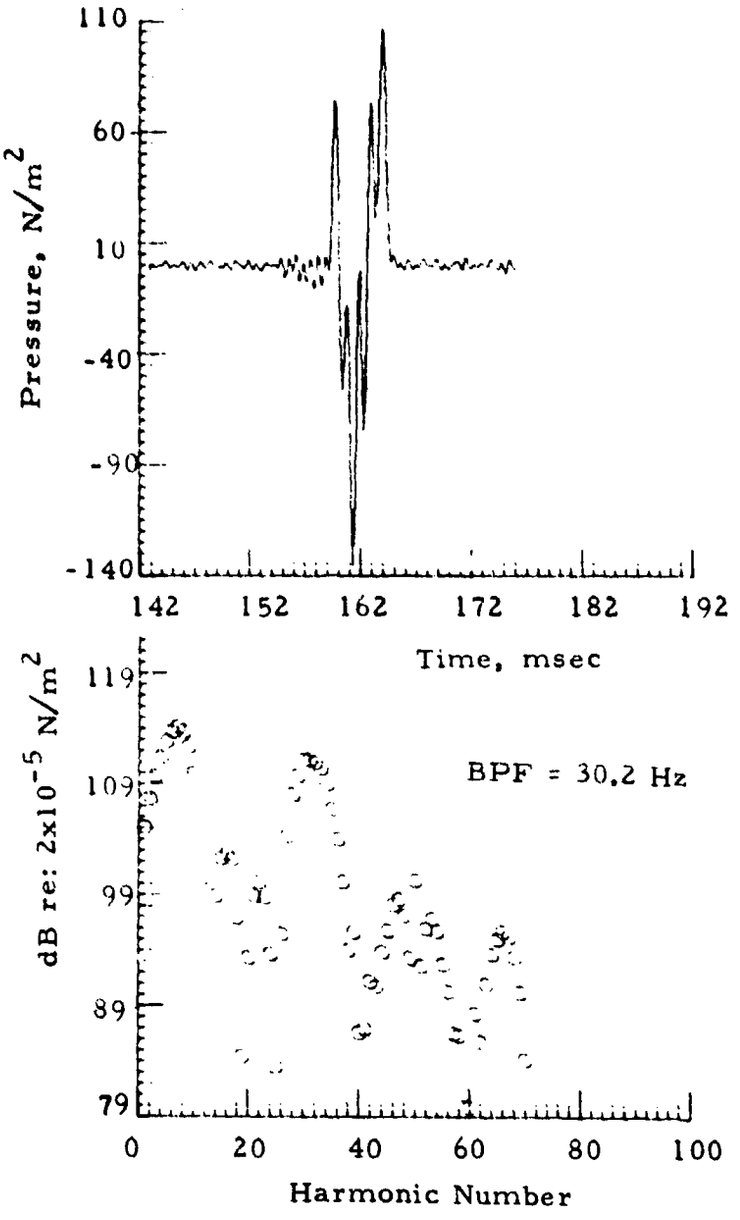

Figure 3. Example 3.- Theoretical acoustic pressure signature and spectrum of a hovering helicopter rotor for an observer in the plane of rotation. Tip Mach number = 1.375.

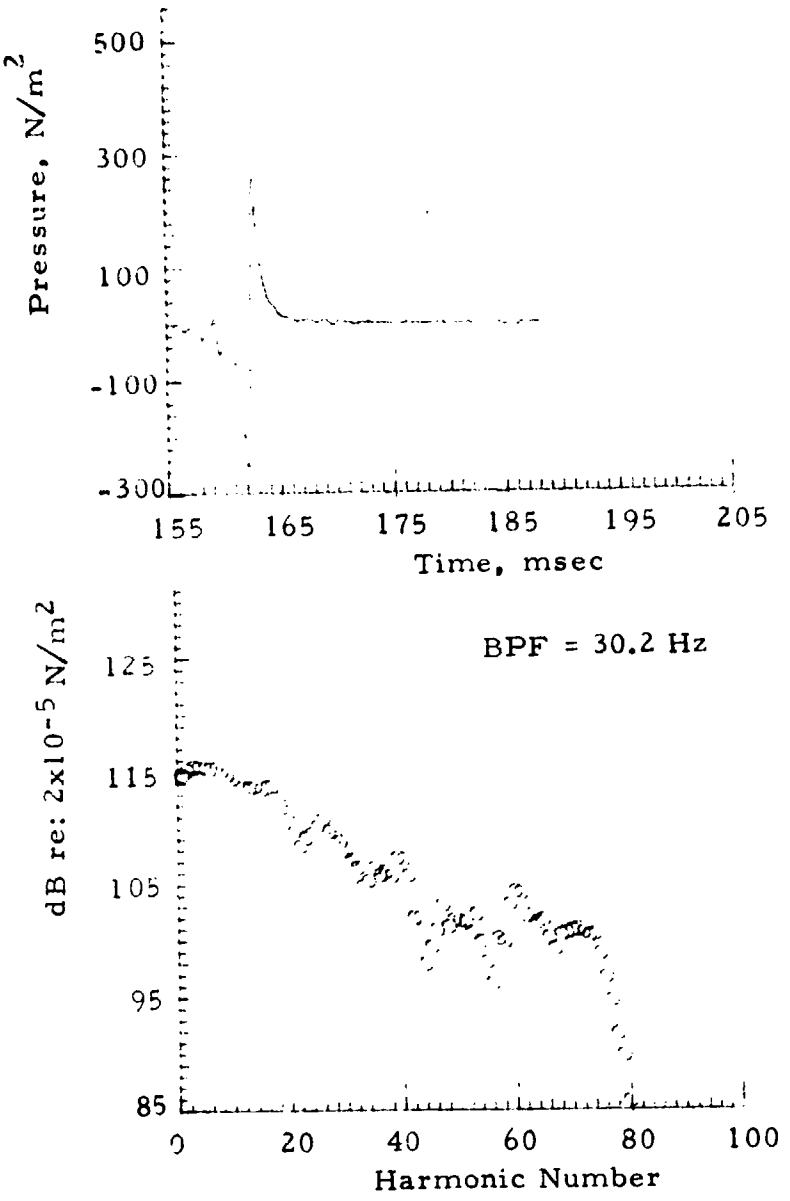

Figure 4. Example 4.- Theoretical acoustic pressure signature and spectrum of a hovering helicopter rotor for a observer at 45° elevation above rotor plane. Tip Mach number 1.375.

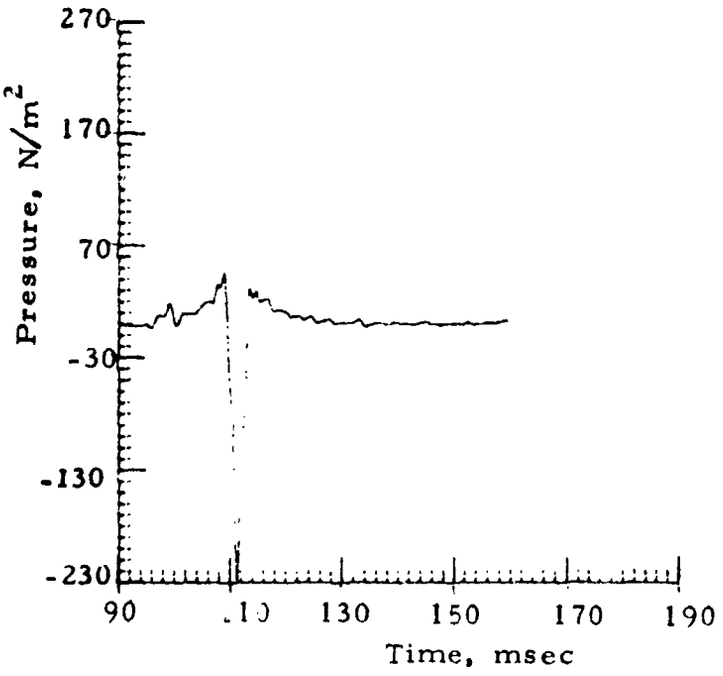

Figure 5. Example 5.- Theoretical acoustic pressure signature (thickness noise only) of a helicopter in forward flight (59.2 m/sec, 115 kts) for an observer 2° below the rotor plane. Advancing tip Mach number = 0.90.